XII. GEOPHYSICAL RESEARCH*

Research Staff

Dr. G. W. Grams
Dr. W. D. Halverson
J. B. Thompson

Graduate Students

S. J. Bless
J. B. DeWolf

RESEARCH OBJECTIVES

The work of our group is being carried out as a cooperative effort with Giorgio Fiocco, of the European Space Research Institute (ESRIN), Frascati, Italy. For the most part, this research is directed toward problems of interest in the atmospheric sciences. In particular, we have conducted spectral analyses of the light scattered from a laser beam by atmospheric molecules and aerosols, using a Fabry-Perot interferometer to measure the spectral distribution of the scattered light. These experiments have provided measurements of the ratio of aerosol-to-molecular scattering for naturally occurring aerosols in the laboratory air and for artificially produced fogs.[1] The experiments will continue with interferometers of greater spectral resolution, with the aim of deriving the temperature of the atmosphere from the observed spectral-line profiles of the scattered light.

An investigation of the effect of turbulence and aerosol diffusion on the spectrum of scattered laser radiation has also been initiated. Some experimental data of the spectrum of light scattered by small particles in a submerged water jet have been obtained. This research is being performed out by J. B. DeWolf, and preliminary results of the experiments are presented in Section XII-A.

Analyses of data from previous optical radar experiments continue and new results have been reported.[2,3] At the present time, G. Fiocco and G. W. Grams are working on a theoretical model for the seasonal variation of the meridional distribution of dust in the upper atmosphere. A preliminary analysis of optical radar data obtained during 1964 and 1965 indicates that the seasonal variation of the dust content of the mesosphere can be interpreted through the use of the theoretical model.

Experiments are being performed with a device that utilizes the effects of pulsed, intense magnetic fields to produce high pressures in solids. The magnetic-pinch apparatus will be used by S. J. Bless to investigate phase stabilities of materials of geophysical interest. Evidence is presented in Section XII-B that pressures exceeding 130 kilobars have been achieved with the device.

Measurements of electron temperature and density in a reflex discharge with the use of a continuous-wave laser and synchronous detection schemes have been completed, and the results of these experiments have been reported.[4,5]

G. W. Grams

*This work was supported principally by the National Aeronautics and Space Administration (Grants NGR-22-009-131 and NGR-22-009-114), and in part by the Joint Services Electronics Programs (U. S. Army, U. S. Navy, and U. S. Air Force) under Contract DA 28-043-AMC-02536(E).

References

1. G. Fiocco and J. B. DeWolf, "Frequency Spectrum of Laser Echoes from Atmospheric Constituents and Determination of the Aerosol Content of Air," J. Atmos. Sci. 25, 488-496 (1968).

2. G. Fiocco, "Possibility of Continuous Measurement of the Influx on Earth of Extraterrestrial Dust by Optical Radar" (NASA Sp-150 (1967), a paper presented at the International Symposium on the Zodiacal Light and the Interplanetary Medium, University of Hawaii, 29 January-2 February 1967).

3. G. Fiocco and G. W. Grams, "Optical Radar Observations of Mesospheric Aerosols in Norway during the Summer 1966" (to appear in J. Geophys. Res.).

4. H. C. Koons and G. Fiocco, "Anisotrophy of the Electron Velocity Distribution in a Reflex Discharge Measured by Continuous-Wave Laser Scattering," Phys. Letters 26A, 614-615 (6 May 1968).

5. H. C. Koons and G. Fiocco, "Measurements of the Density and Temperature of Electrons in a Reflex Discharge by Scattering of cw Ar^+ Laser Light," J. Appl. Phys. 39, 3389-3392 (1968).

A. SPECTRUM OF COHERENT LIGHT SCATTERED FROM A TURBULENT JET

It has been thought that information about turbulence and aerosol diffusion might be obtained by studying the spectrum of the light scattered by the aerosols with the use of an optical homodyne spectrometer.[1] A preliminary study using a steam jet showed, however, that the homodyne spectrum was masked by intensity fluctuations caused by intermittent behavior and density fluctuations in the jet. Fluctuation spectra of this sort have been observed by Becker, Hottel, and Williams.[2] In order to clarify the situation and to see if a homodyne spectrum could be obtained from a turbulent fluid, a study was begun of the spectrum of coherent light scattered from a water jet marked by uniform spherical particles. This portion of the report will summarize what has been learned thus far, by using the turbulent water jet.

The homodyne spectrum gives information about the density correlation function of the particles.[3] It is observed by measuring with a wave analyzer the low-frequency spectrum of the current from a photomultiplier tube which is illuminated by the scattered light. In order to interpret the observed spectrum simply in terms of a density correlation function, the following conditions should be satisfied.

a. The fluctuations in scattered light intensity caused by a change in the total number of scattering particles within the volume should be small. In order to determine whether or not this is the case, it is useful to measure the photocurrent spectrum when incoherent light is used as the source. The homodyne spectrum is only observable with a laser source.

b. The turbulence should be statistically stationary over the time of the measurement.

c. The volume that is observed should be large enough so that the broadening caused by the finite lifetime of the scattering from a particle moving through the volume can be neglected. If the mean velocity of the particles is v, and the width of the homodyne spectrum that is to be observed is Δf, then the size of the scattering volume L should satisfy

$$L \gg \frac{v}{\Delta f}.$$

This may be the major source of broadening in experiments in which the mean velocity of the fluid is large or the scattering volume small.

d. Ideally, the volume that is observed should be small enough so that the mean velocity of the fluid is essentially constant within the volume. This is desirable so that the density correlation function will be more or less homogeneous over the scattering volume.

Some measurements of the spectrum of light scattered by particles suspended in a submerged water jet have been made in such a way that these conditions are reasonably well satisfied. The jet emerges from a nozzle, 1 mm in diameter, into a glass-walled circular duct, 5.33 cm in diameter. Both the water emerging from the jet and the water in the duct are marked with uniform latex spherical particles having a diameter of 910 Å ± 58 Å. The jet can be moved relative to the laser beam and the photomultiplier in such a way that the position of the scattering volume can be precisely located with respect to the center line of the jet and the nozzle. The flow rate is measured with a calibrated flowmeter. The homodyne spectrometer is similar to the one described by Dubin, Lunacek, and Benedek.[2] The photocathode is at right angles to the laser beam.

A detailed analysis of the data has not yet been completed, but the following general picture emerges.

First, when the jet is turned off the particles undergo Brownian motion. The density correlation function and the spectrum of the light observed in this case are well understood. The line shape is Lorentzian and has a width that is proportional to the diffusion coefficient. Since the diffusion coefficient for the uniform spherical particles can be calculated from the Stokes-Einstein relation, the width of the spectrum can be calculated and compared with experiment. Figure XII-1 shows the spectrum of the light observed when the jet is turned off. The solid curve is a Lorentzian having a width of 0.674 kHz, which agrees well with the calculated value.

Second, when the jet is turned on, the spectrum of the light scattered from the jet region is observed to broaden. It is inferred that the broadening of the spectrum is caused by an increase in the effective diffusion coefficient because of the turbulence. The observed spectrum maintains a Lorentzian shape, at least initially, as the jet velocity increases. Figure XII-2 shows the spectrum of the light observed 40 nozzle diameters downsteam from the nozzle on the axis of the jet when the nozzle velocity is

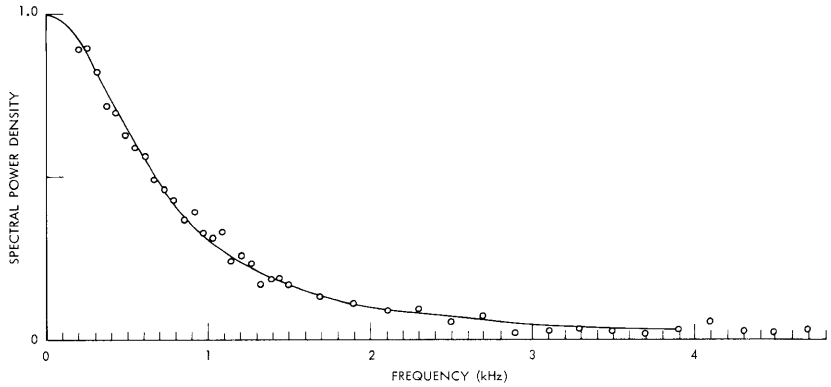

Fig. XII-1. Spectrum of light scattered from spheres of 910 Å diameter undergoing Brownian motion in a water solution. Solid curve is Lorentzian with 674-Hz width.

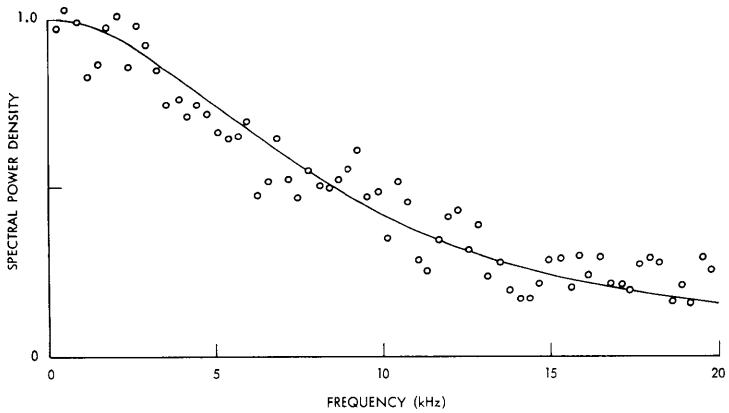

Fig. XII-2.

Spectrum of light scattered from spheres of 910 Å diameter suspended in a turbulent water jet. Scattering volume is on axis, 40 nozzle diameters downstream from the nozzle. Flow rate: 20 ml/min. Solid curve is Lorentzian with 8.48-kHz width.

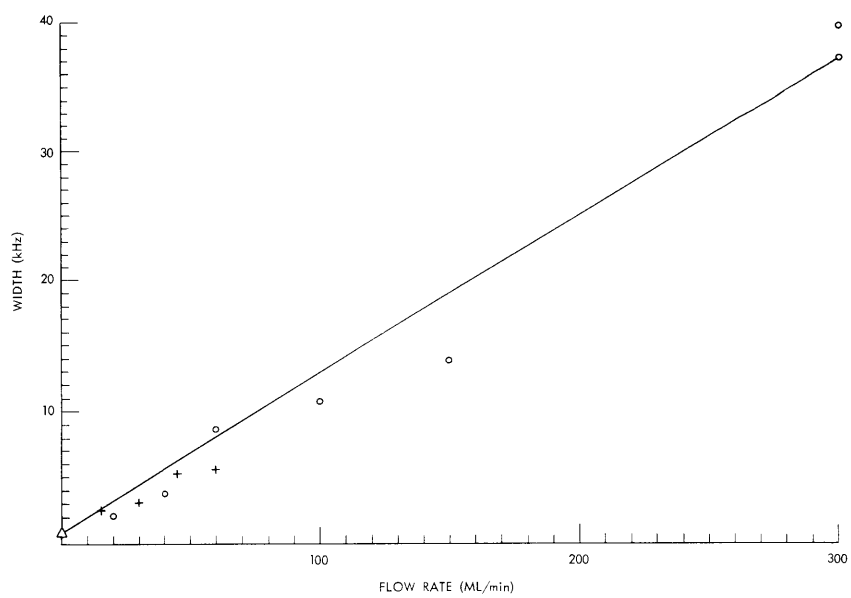

Fig. XII-3. Width of the scattered spectrum as a function of jet flow rate. Data were taken on the axis of the jet, 80 nozzle diameters downstream from the nozzle.

approximately 42 cm/sec. The curve has a width of approximately 8.5 kHz. Figure XII-3 shows the width of the spectrum as a function of the flow rate in the jet when the scattering volume is 80 nozzle diameters downstream from the nozzle on the jet axis.

Third, as the scattering volume is moved radially, the width of the spectrum decreases until the minimum width (caused by the equilibrium Brownian motion) is reached. This behavior has been examined as a function of the distance from the nozzle and it is possible to observe in this fashion the spreading of the jet with increasing distance from the nozzle.

Further analysis is being undertaken in the hope that information about the kinetics of turbulent diffusion may be obtained in this manner.

J. B. DeWolf

References

1. S. B. Dubin, J. H. Lunacek, and G. B. Benedek, "Observation of the Spectrum of Light Scattered by Solutions of Biological Macromolecules," Proc. Natl. Acad. Sci. U.S. 57, 1164-1171 (1967).
2. H. A. Becker, H. C. Hottel, and G. C. Williams, "On the Light-Scatter Technique for the Study of Turbulence and Mixing," J. Fluid Mech. 30, 259-284 (1967).
3. G. Fiocco and J. B. DeWolf, "Frequency Spectrum of Laser Echoes from Atmospheric Constituents and Determination of the Aerosol Content of Air," J. Atmos. Sci. 25, 488-496 (1968).

B. HIGH-PRESSURE EXPERIMENTS WITH A MAGNETIC PINCH

1. Introduction

Modern high-pressure research has been applied to several geophysical problems. Experiments with static pressure devices have been successful in duplicating the pressure and temperature regimes of the crust and upper mantle. In the lower mantle and core, pressures of 400 kbar to 3600 kbar and temperatures of 1500-6000°K are encountered. Static devices have been unable to produce pressures greater than 500 kbar, and the pressure-temperature relation of the Earth can only be reproduced to 100 kbar. Shock waves, however, are able to produce pressures as high as 5 Mbar. Although the pressure-temperature relationship cannot be varied in shock waves, it is believed to be similar to that of the Earth. The disadvantages of shock compression are one-dimensional strain and short duration. Because of these difficulties, we have been working on a new means of pressure production, utilizing an electric pinch. This method may be useful in supplementing shock-wave data in the range 100-500 kbar.

2. Apparatus

Energy is stored in eight 15-μF, 3000-J, 20-kV capacitors. The discharge circuit used in these experiments is essentially the same as that described in a previous report.[1] Figure XII-4 is a schematic drawing of one capacitor circuit. The inductance

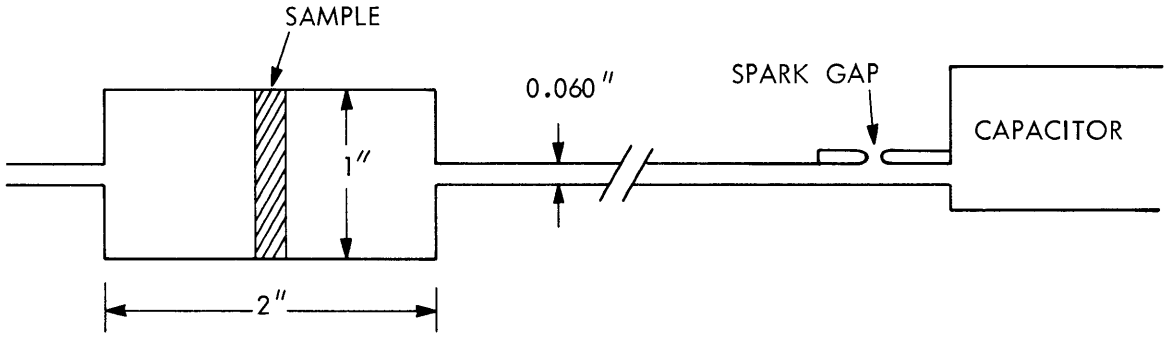

Fig. XII-4. Geometry for inductance calculation.

calculated from this geometry is 13.6 nH for a sample 4 mm in diameter. The inductance of the spark gaps is estimated to be 6.7 nH, and the rated inductance of the capacitors is 5 nH.

The resistance of the sample is given by

$$R_s = \frac{\rho \ell}{\pi s(r-s)},$$

where ρ is the resistivity, ℓ is the length (1 in.), r is the radius, and s is the skin depth. In these experiments, $R_s \lesssim 0.1\ \omega L$ and hence the discharge period is given by

$$T = 2\pi\sqrt{NC_oL}, \tag{1}$$

with L = 25.3 nH (for a 4-mm diameter sample), C_o = 15 μF, and N = the number of capacitors employed.

The pinch pressure is

$$P = B^2/2\mu_o$$

$$P_{max} = \frac{2\mu_o N^2 C_o^2 V^2}{T^2 d^2}$$

$$= \frac{\mu_o N C_o V^2}{2\pi^2 L d^2}. \tag{2}$$

In Eq. 2, V is the initial voltage on the capacitors, d is the sample diameter, and $\mu_o = 4\pi \times 10^{-7}$ H/m.

Equations 1 and 2 have been evaluated for N = 1 to 8, d = 2 mm and 4 mm, and V = 20 kV. The resulting peak pressures are shown in Fig. XII-5.

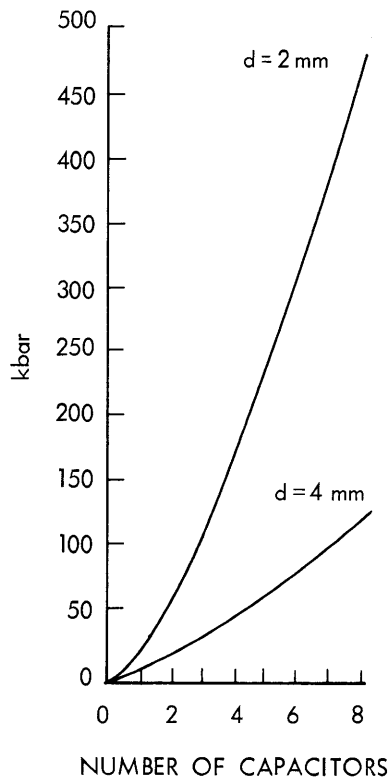

Fig. XII-5. Maximum pressure possible in rods of 2 mm and 4 mm diameter. Calculated from Eqs. 1 and 2.

3. Energy Deposition

In the first experiments, under the supervision of Professor Francis Bitter, we studied the effect of the discharge on molybdenum and stainless-steel rods of various diameters. At that time, only 4 capacitors were available, thereby limiting the energy to 12,000 J (2870 cal). Only 6 sizes of rods were used; they were loosely confined in boron nitride cylinders of 7.15-mm diameter. Figure XII-6 shows how the discharge affected the rods. Figures XII-7 and XII-8 show the results of investigations at higher energies.

The experimental results shown in Figs. XII-6 through XII-8 seem to justify the following conclusions.

(i) Unless the rod is broken, only a small portion of the energy in the capacitor bank is deposited in it.

(ii) Complete vaporization of 4-mm rods is energetically impossible, even when the

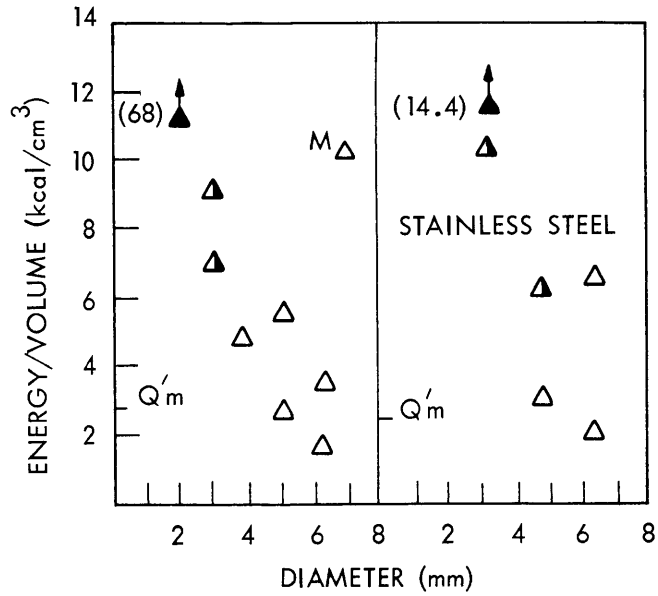

Fig. XII-6. Effect of the discharge on molybdenum and stainless-steel rods. Open triangles represent very little damage, half-open triangles are badly damaged but not broken, filled triangles represent complete destruction. Q'_m is the energy required to melt the rods (2.87 kcal/cm^3).

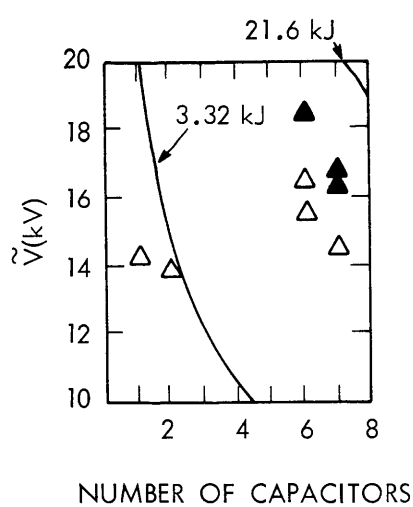

Fig. XII-7.

Effect on 4-mm diameter annealed, tightly confined Armco iron rods. The energies required to melt and vaporize the rod are shown.

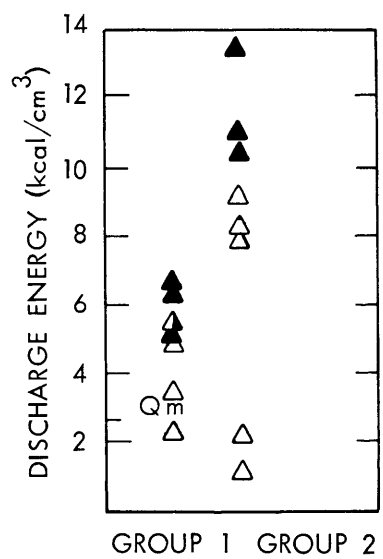

Fig. XII-8.

Effects on all 4-mm diameter iron rods. Group 1 were neither annealed nor confined. Group 2 are those shown in Fig. XII-7. Q'_m is the specific energy required to melt the rods.

rod is completely destroyed.

(iii) The effect of confinement on a rod is to increase the energy required to destroy it.

The first of these conclusions can be explained theoretically by adopting a model in which the current progressively melts outer layers of the rod and moves inward. Let

$$Z_1(r) = R_s + \omega L_s$$

equal the impedance for conduction through a solid rod of radius r, with R_s and L_s the resistance and inductance of the sample. Let $s = \sqrt{\frac{\rho}{\pi\mu_o\nu}}$ be the classical skin depth. Then

$$Z_1(r) = \frac{\rho\ell}{\pi s(2r-s)} + \omega L_s(r).$$

The impedance for conduction through a melted cylindrical shell of outer radius r_o and inner radius r is

$$Z_2(r) = \begin{cases} \dfrac{\rho_m \ell}{\pi s(2r_o - s)} + \omega L_s(r_o) & \text{for } r_o - r > s \\[2ex] \dfrac{\rho_m \ell}{\pi\left(r_o^2 - r^2\right)} + \omega L_s(r_o) & \text{for } r_o - r < s. \end{cases} \tag{3}$$

In order to evaluate (3), the resistivity for liquid iron at high temperatures must be known. F. D. Bennett[2] obtained the resistivity for an exploding copper wire as a function of specific energy; ρ_m did not increase much above 150×10^{-8} Ω-m until vaporization began. Therefore, the use of the handbook value of the resistivity of liquid iron, 139×10^{-8} Ω-m,[3] seems justified in this case.

Figure XII-9 represents a graphic solution of the equation $Z_1(r) = Z_2(r)$ for two different values of T. In both cases the solution, r_c, is slightly underestimated because the increase in the resistivity of solid iron with temperature has not been taken into account. Since r_c is much greater than zero, it has been demonstrated that the current will be shunted by the outer melted material after a small penetration into the solid rod. This explains why the entire rod is not melted.

The explanation for conclusions (ii) and (iii) could be that instabilities in the plasma sheath formed around the rod are chiefly responsible for its destruction. When the rods are confined, the plasma is suppressed. Destruction occurs if the scale of plasma instabilities reaches a critical size and can overcome the strength of the rod. Several exploding-wire observations support this hypothesis.[4]

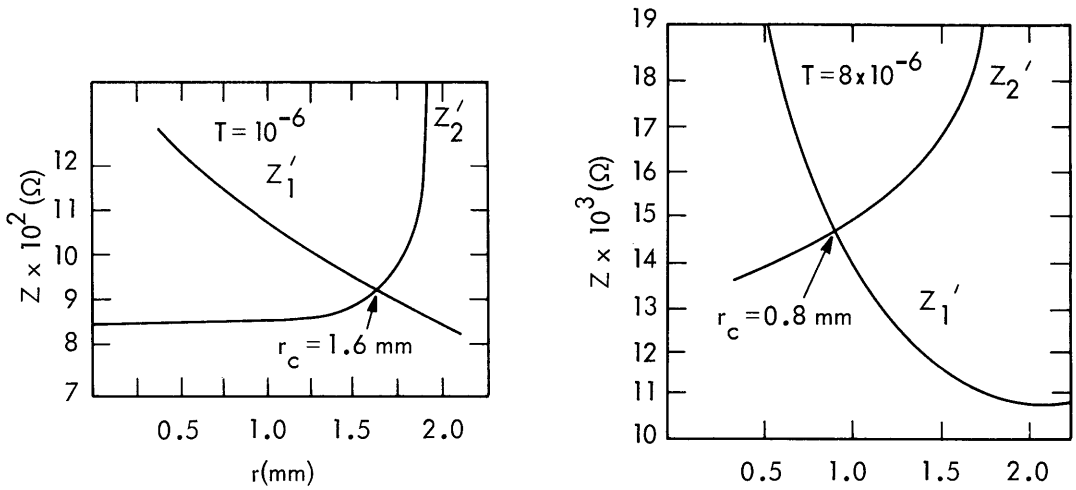

Fig. XII-9. Solution of $Z_1(r) = Z_2(r)$.

4. Experiments with Iron

Figure XII-10 illustrates the phase diagram for iron. We have attempted to produce the high-pressure ϵ phase with magnetic pinch pressure. The $\alpha \rightarrow \epsilon \rightarrow \alpha$ transition sequence can be identified by the restructuring of the ferrite grains that accompanies recrystallization.[1,5,6]

Many experiments were carried out with annealed and unannealed iron rods,

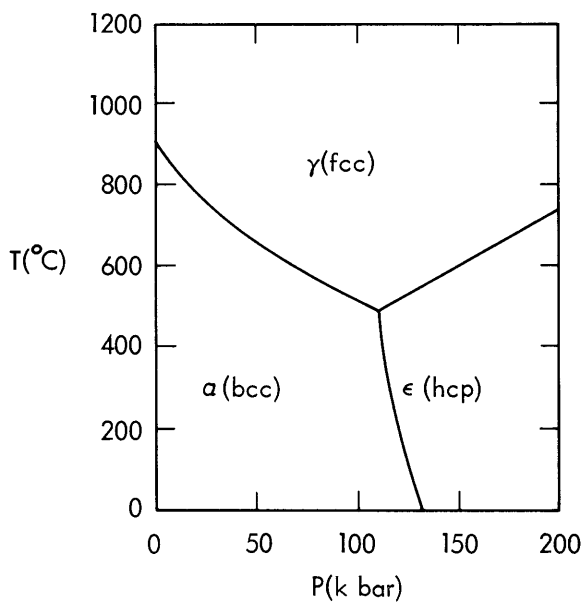

Fig. XII-10. Phase diagram of iron.

4 mm in diameter and 1 inch long. Figure XII-5 and the solution to Eq. 3 indicate that pinch pressures in excess of 130 kbar may be produced in such rods. The maximum energy that the rods could absorb is shown in Fig. XII-8.

Evidence for a phase transition was obtained in two rods. In a previous report[1] we have given the results for an unannealed rod. Figures XII-11 and XII-12 illustrate the result for an annealed rod.

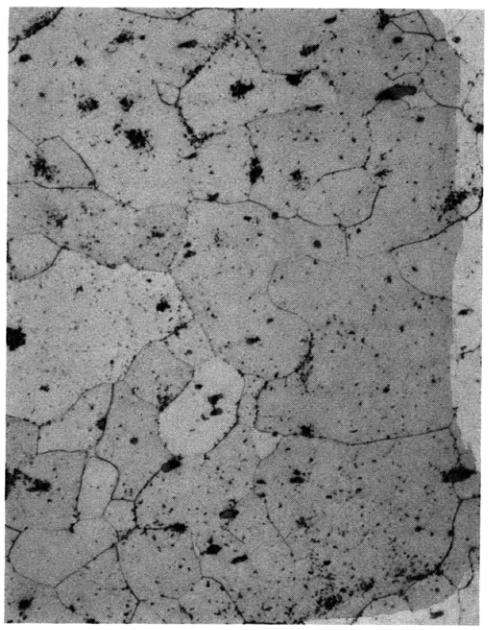

Fig. XII-11. 4-mm annealed iron rod (100X).

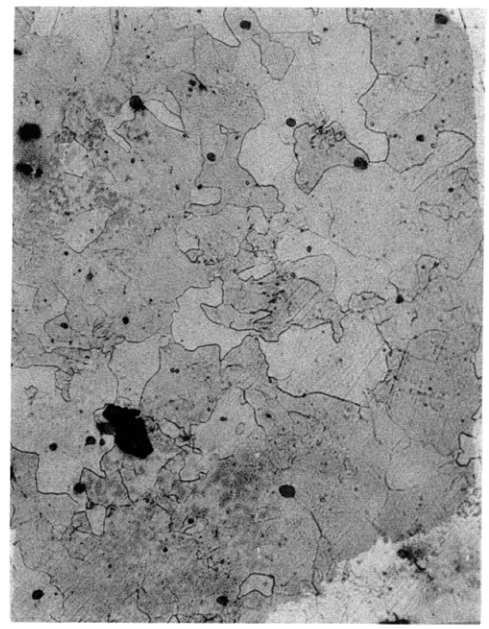

Fig. XII-12. 4-mm annealed rod after discharge (6 capacitors, 16.5 kV, 100X).

The probability that the $\alpha \rightarrow \gamma \rightarrow \alpha$ transition sequence has occurred (rather than $\alpha \rightarrow \epsilon \rightarrow \alpha$) is small for the following reasons.

1. Rods that were fired at slightly less energy than the one shown in Fig. XII-12 showed no evidence of recrystallization, even near the surfaces.

2. In a region adjacent to the copper electrode (which was partially melted) clear effects of the $\alpha \rightarrow \gamma \rightarrow \alpha$ sequence were observable. These included impurity precipitation at grain boundaries which is absent in Fig. XII-12.

3. There is insufficient time for the rod to heat, since

$$\frac{\partial T}{\partial t} = \frac{\alpha}{r} \frac{\partial}{\partial r} \left(r \frac{\partial T}{\partial r} \right)$$

$$\frac{\Delta T}{\Delta t} \approx \bar{\alpha} \frac{T_{max}}{\Delta x^2}, \tag{4}$$

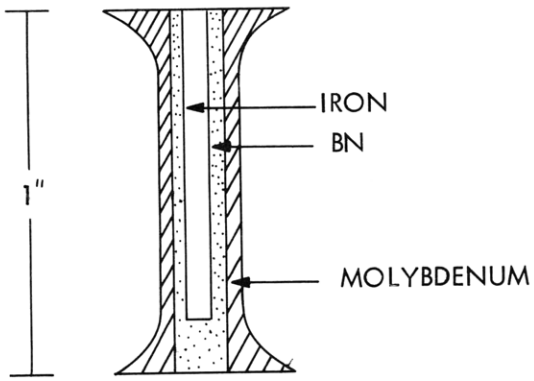

Fig. XII-13. Insulated iron sample.

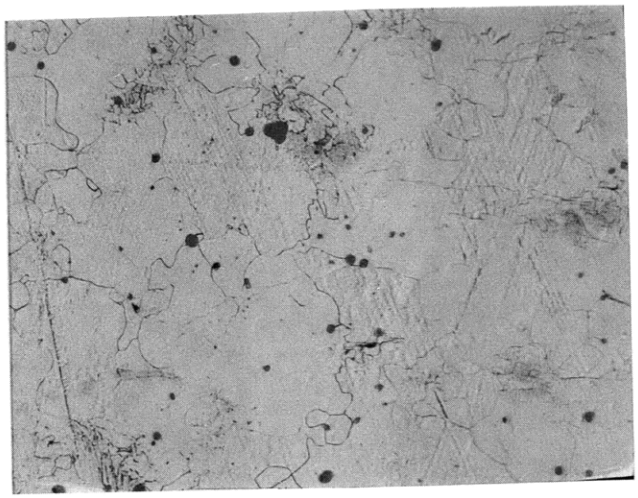

(a)

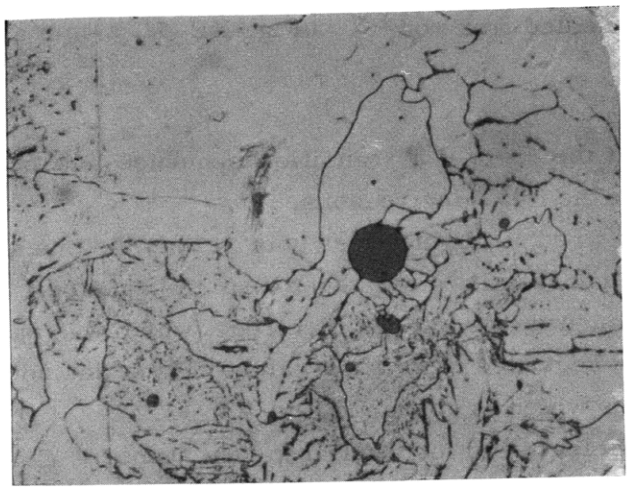

(b)

Fig. XII-14. Iron interior of sample shown in Fig. XII-13 after discharge (8 capacitors, 18 kV). (a) 100X; (b) 500X.

with $\bar{\alpha} \approx 0.10\ cm^2/sec$, $T_{max} \lesssim 5000°C$ (see Shanks[7]), $\Delta x \approx 0.1$ cm. Hence

$$\frac{\Delta T}{\Delta t} \approx 5 \times 10^4 °C/sec.$$

Since $\Delta t < 10^{-3}$ sec, $\Delta T < 50°C$.

In an attempt to further exclude the possibility of the rod getting hot enough for the $\alpha \rightarrow \gamma$ transition to occur, insulated samples, as shown in Fig. XII-13, were constructed.

Figure XII-14 shows the microstructure of this iron rod after a pinch discharge. Again, there is evidence for a phase transition. In this case, $\Delta T/\Delta t$ calculated from Eq. 4 is only 7800°C/sec.

5. Additional Experiments

Experiments have also been carried out with boron nitride and fused quartz rods. These materials were coated with a conducting metal. The high-pressure wurtzite and zinclend phases of BN were sought,[3] but no evidence for their production was obtained. Similarly, no crystalline phases of quartz were produced by the pinch. In both cases, failure to synthesize high-pressure forms may be accounted for by the sluggishness of the recrystallization processes.

S. J. Bless

References

1. F. Bitter, S. J. Bless, and G. Fiocco, "Preliminary Experiments with a Fast z-pinch Capacitor Discharge: The Generation of High Pressures in Solids," Quarterly Progress Report No. 86, Research Laboratory of Electronics, M. I. T., July 15, 1967, pp. 53-57.
2. F. D. Bennett et al., "Resistance Changes Caused by Vaporization Waves in Exploding Wires," Exploding Wires, Vol. 3, W. G. Chace and H. K. Moore (eds.), pp. 65-88, 1964.
3. Metals Handbook, Vol. L (American Society for Metals, 8th edition, 1961).
4. F. P. Bundy and R. H. Wentorf, "Direct Transformation of Boron Nitride to Denser Forms," J. Chem. Phys. 38, 1144-49 (1963).
5. P. C. Johnson et al., "Temperature Dependence of Shock-Induced Phase Transformation in Iron," J. Appl. Phys. 33, 557-61 (1962).
6. C. S. Smith, "Metallographic Studies of Metals after Explosive Shock," Trans. Met. Soc. AIME, pp. 574-588, October 1958.
7. H. R. Shanks et. al., "Thermal Properties of Armco Iron," J. Appl. Phys. 38, 2805-2892 (1967).